Biochemistry

 Volume 39, Number 20 May 23, 2000

Articles

Reaction of Bovine Cytochrome *c* Oxidase with Hydrogen Peroxide Produces a Tryptophan Cation Radical and a Porphyrin Cation Radical†

Stephen E. J. Rigby,‡ Susanne Jünemann,§ Peter R. Rich,§ and Peter Heathcote*,‡

School of Biological Sciences, Queen Mary and Westfield College, University of London, Mile End Road, London E1 4NS, U.K., and The Glynn Laboratory of Bioenergetics, Department of Biology, University College London, University of London, Gower Street, London WC1E 6BT, U.K.

Received November 11, 1999; Revised Manuscript Received February 2, 2000

ABSTRACT: Oxidized bovine cytochrome *c* oxidase reacts with hydrogen peroxide to generate two electron paramagnetic resonance (EPR) free radical signals (Fabian, M., and Palmer, G. (1995) *Biochemistry 34*, 13802−13810). These radicals are associated with the binuclear center and give rise to two overlapped EPR signals, one signal being narrower in line width (ΔHptp = 12 G) than the other (ΔHptp = 45 G). We have used electron nuclear double resonance (ENDOR) spectrometry to identify the two different chemical species giving rise to these two EPR signals. Comparison of the ENDOR spectrum associated with the narrow signal with that of compound I of horseradish peroxidase (formed by reaction of that enzyme with hydrogen peroxide) demonstrates that the two species are virtually identical. The chemical species giving rise to the narrow signal is therefore identified as an exchange-coupled porphyrin cation radical similar to that formed in horseradish peroxidase compound I. Comparison of the ENDOR spectrum of compound ES (formed by the reaction of hydrogen peroxide with cytochrome *c* peroxidase) with that of the broad signal indicates that the chemical species giving rise to the broad EPR signal in cytochrome *c* oxidase is probably an exchange coupled tryptophan cation radical. This is substantiated using H_2O/D_2O solvent exchange experiments where the ENDOR difference spectrum of the broad EPR signal of cytochrome *c* oxidase shows a feature consistent with hyperfine coupling to the exchangeable N(1) proton of a tryptophan cation radical.

Cytochrome *c* oxidase (C*c*O)[1] catalyses the transfer of electrons from ferrocytochrome *c* to oxygen and the coupling of this redox reaction to the pumping of protons across the inner mitochondrial or bacterial membrane. The catalytic mechanism of oxygen reduction to water at a binuclear center containing heme a_3 and Cu_B includes two-electron-reduced intermediate (**P**eroxy) and a three-electron-reduced (oxo**F**erryl) intermediate, which were first observed as two distinct spectral forms of C*c*O at 607 nm (**P**) and 580 nm (**F**) following reversal of electron transfer from water to cyto-

† This work was supported by supported by grants from an European Union TMR programme (to P.H. Contract Number FMRX-CT98-0214) and from the Wellcome Trust (to P.R.R., ref 049722/Z).

* To whom correspondence should be addressed.
‡ Queen Mary and Westfield College.
§ University College London.

[1] Abbreviations: CO, carbon monoxide; C*c*O, cytochrome *c* oxidase; C*c*P, cytochrome *c* peroxidase; ΔHptp, line width peak-to-peak of first derivative EPR spectrum; DFT, density functional theory; ENDOR, electron nuclear double resonance; EPR, electron paramagnetic resonance; hfc, hyperfine coupling; HRPC, horseradish peroxidase, isoform C; rf, radio frequency.

10.1021/bi992614q CCC: $19.00
Published on Web 04/26/2000

chrome (*1*−*3*). Species related to **P** and **F** (including **F**•; see below) are also observed following the addition of hydrogen peroxide (H_2O_2) to oxidized C*c*O (*4*−*7*). In **P** species produced by reaction of oxidized C*c*O with H_2O_2 (*8*), and by reaction of the mixed-valence (*9*) and fully reduced enzyme (*10*) with oxygen, resonance Raman spectra exhibited a mode characteristic of Fe^{IV}═O. This suggests that the O−O bond is broken in both the **P** and **F**• forms. The reductive cleavage of this bond requires three electrons relative to the oxidized state, but only two electrons can be provided by the metal centers at the **P** or **F**• stage of the oxygen reduction cycle.

A number of different states have been proposed to account for the additional electron: (a) the further oxidation of heme a_3 to Fe_{a3} (V) (*9*); (b) the further oxidation of Cu_B to Cu(III) (*11*); (c) the donation of the electron from the heme a_3 macrocycle to form a porphyrin π cation radical as happens, for example, in ascorbate peroxidase (*12*) and catalase (*13*, *14*); (d) oxidation of an amino acid to form a radical, as has been reported in prostaglandin H synthase (*15*) and cytochrome *c* peroxidase (C*c*P) (*16*).

The crystal structures of the cytochrome oxidases from bovine heart (*17*) and *Paracoccus denitrificans* (*18*) show a tyrosine residue close to the binuclear center which is covalently cross-linked to one of the histidine ligands of Cu_B. It has been suggested that this tyrosine could be oxidized to provide the fourth electron required for O−O bond cleavage (*9*, *18*, *19*−*21*).

P and **F** species related to the **P** and **F** intermediates of C*c*O are thought to be formed consecutively by the reaction of two molecules of hydrogen peroxide with oxidized C*c*O. The extent and rate of the reaction, and the ratio of the two forms, depend on pH and H_2O_2 concentration (*4*, *7*, *11*). In a recent kinetic analysis of the reaction of oxidized C*c*O with H_2O_2 (*19*) in the pH range 6.0−9.0 we have found a more complex situation, where a 580 nm species termed **F**• can be formed by reaction with a single H_2O_2 at low pH, as previously reported for the *bo* quinol oxidase from *Escherichia coli* (*20*). However in bovine oxidase it seems that **P** and **F**• are not in a rapid pH-dependent equilibrium, since lowering the pH of a sample containing $\mathbf{P_H}$ (the species formed by reaction with H_2O_2) and $\mathbf{P_M}$ (formed by reaction with CO/O_2) only results in formation of **F**• on a time scale of minutes. It was concluded that **P** and **F**• are not in a rapid, pH-dependent equilibrium, but instead are formed by distinct pathways and cannot interconvert in a simple manner, and that the crucial difference between them lies in their patterns of protonation.

Two EPR radical signals have been observed following the incubation of cytochrome *c* oxidase with H_2O_2 (*11*), although at low occupancy (less than 0.1 spin per enzyme). We observed in our studies (*19*) similar radicals, which were not observed in samples pretreated with cyanide or formate or exposed to CO and must therefore be associated with the binuclear center. The different microwave power saturation behaviors of these two radicals indicates they arise from two distinct species, but there was no clear correlation between their levels and those of any intermediate (**P**, **F**•, or **F**).

Electron nuclear double resonance (ENDOR) spectroscopy is a paramagnetic resonance technique that can detect the hyperfine couplings between the unpaired electron in free radical and the magnetic nuclei in the chemical species. As a result, it can be used to identify the chemical species giving rise to the EPR free radical signal and to probe the electronic structure of the radical and its interaction with the surroundings. We have used this technique to study the two free radicals generated by the interaction of H_2O_2 with oxidized C*c*O and demonstrated that they arise from a porphyrin cation radical and a tryptophan cation radical. During the preparation of this manuscript a paper by MacMillan et al. (*21*) reported that only one free radical species, attributed to a tyrosine radical, was found on reaction of *Paracoccus denitrificans* C*c*O with H_2O_2.

MATERIALS AND METHODS

Bovine C*c*O oxidase was prepared by a procedure (*22*) which yields "fast" enzyme with monophasic cyanide binding kinetics and a characteristic Soret maximum at 424 nm. The concentration was determined optically from the dithionite-reduced *minus* oxidized difference spectrum using an extinction coefficient of $\Delta\epsilon_{606-621\ nm} = 25.7\ mM^{-1}cm^{-1}$ (*23*).

The H_2O_2 stock was a 30% (w/v) stabilized solution, i.e., equivalent to 9.7 M H_2O_2, which was stored at 4 °C. Dilutions were prepared in double-distilled water and calibrated optically using an extinction coefficient at 240 nm of 40 $M^{-1}\ cm^{-1}$ (*24*). Values agreed with concentrations determined by measurement of the oxygen evolved when the solution was added to 50 mM potassium phosphate pH 7.5 containing 10^4 U/mL catalase in a Clarke-type electrode. Diluted solutions were kept on ice and used within 4 h.

C*c*O (100 μM) was suspended in 0.1 M MES buffer pH 6.5 containing 0.05% (w/v) lauryl maltoside and 100 units/ml superoxide dismutase. A 1 mM H_2O_2 solution was added and the sample frozen in liquid nitrogen after 3 min (*19*). To exchange oxidase into D_2O, oxidase was spun down and resuspended in D_2O at pD 8.5. It was incubated overnight at 4 °C and concentrated by centrifugation. The sample was checked to ensure it was still a "fast" enzyme and then incubated as above with 0.5 mM H_2O_2 before freezing in liquid nitrogen. A control C*c*O sample was prepared in the same way at pH 8.5 in 0.1 M Tricine buffer. Attempts to exchange the C*c*O into D_2O at pH 6.5 inevitably resulted in conversion of a significant amount of oxidase into the "slow" form.

Yeast cytochrome *c* peroxidase (C*c*P) was prepared as in ref 25. Compound ES was prepared by treating the enzyme with H_2O_2 using the conditions described in ref 27 but with 0.1 M MES pH 6.5 as the buffer instead of 10 mM acetate pH 6.0. Horseradish peroxidase (HRPC) (Sigma HRPC, type II) was dissolved to 24 mg/ml in 0.1 M phosphate buffer at pH 7.0 and compound I prepared by the addition of 2.5 mM H_2O_2. After incubation for 40 s, the sample of HRPC was frozen in liquid nitrogen.

ENDOR and EPR spectra were obtained at X-band using a Bruker ESP 300 EPR spectrometer. Acquisition conditions for specific spectra are given in the figure captions. Precision of hfc determination, i.e., the variation in hfc determination between these samples, was ±0.1 MHz. Spectra are presented in first-derivative mode. The hyperfine coupling constants are measured from zero crossing points. However, because of overlap in such relatively crowded spectra it is not always possible to see the zero crossing point for both of the two symmetry-related features (high and low frequency) arising

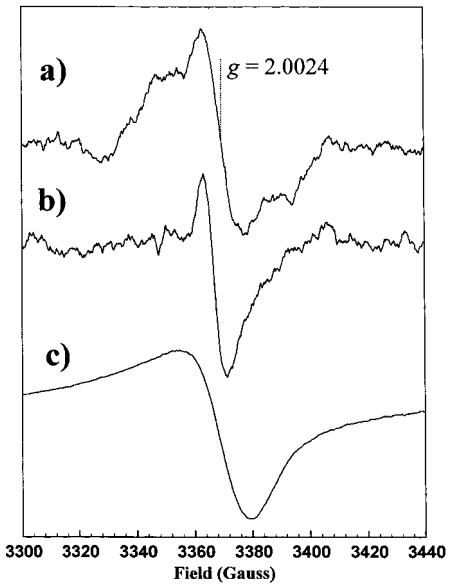

FIGURE 1: EPR spectra of H_2O_2-treated (a) cytochrome *c* oxidase (C*c*O) at pH 6.5 (0.1 M MES buffer), (b) horseradish peroxidase (HRPC) (0.1 M phosphate buffer pH 7.0), and (c) cytochrome *c* peroxidase (C*c*P) (0.1 M Mes buffer pH 6.5). All spectra were recorded in the ENDOR cavity (*Q* factor ~ 800). Preparation conditions given in Materials and Methods. Conditions: microwave power 30 μW; modulation amplitude 1.2 G; modulation frequency 12.5 kHz; temperature 80 K. (a) and b) are the sums of four scans.

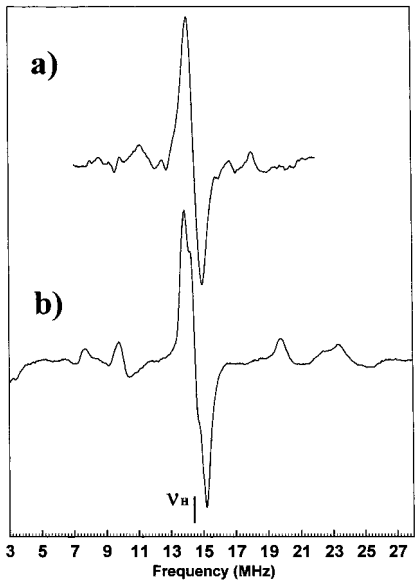

FIGURE 2: ENDOR spectra of H_2O_2-treated cytochrome *c* oxidase at pH 6.5 showing in (a) the spectrum arising from the narrow EPR signal and in (b) the spectrum arising from the broad EPR signal. Conditions: (a) microwave power 3.9 mW; rf power 100 W; rf modulation depth 177 kHz, average of 120 scans, temperature 100 K; (b) microwave power 24 mW, rf power 100 W, rf modulation depth 140 kHz, average of 60 scans, temperature 12 K.

from the same hfc. In these cases the zero crossing point is marked where possible and where this is not possible the point closest to the zero crossing is marked, hence the fact that some arrows appear to indicate troughs and minor inflections. In these cases the hfc is determined by taking *A*/2 as the frequency difference between the observable zero crossing point and the Larmor frequency ν_H.

RESULTS

Figure 1a shows the $g = 2.00$ region of the EPR spectrum of C*c*O treated with 1mM (H_2O_2) at pH 6.5. This spectrum is very similar to those obtained by Fabian and Palmer (*11*) and Jünemann et al (*19*), apparently consisting of two overlapped signals, one with ΔHptp = 12 G and the other with ΔHptp = 45 G. Oxidized Cu_A also gives an EPR signal in these samples (*11, 19*), but this only contributes to a baseline shift in the spectra shown in Figure 1, which are over too narrow a field range to show Cu_A. The relative proportions of these two signals have been shown to vary with pH (*11, 19*), the narrow signal being more abundant at high pH. Figure 1b,c shows the $g = 2.00$ regions of the EPR spectra of other heme proteins treated with H_2O_2, these proteins being HRPC and yeast C*c*P, respectively. Such treatment leads to the formation of states known as compound I in HRPC and compound ES in C*c*P. EPR spectra of these states have been reported previously, for example by Schultz et al. (HRPC) (*26*) and Hoffman et al. (C*c*P) (*27*) and are attributed to a porphyrin cation radical (*28*) and a tryptophan (W191) cation radical (*16*), respectively, both these radicals being spin-coupled to the oxyferryl (Fe^{IV}=O) iron of the heme. The EPR spectrum of compound I of HRPC, with ΔHptp = 10 G, resembles the narrow component of the EPR spectrum from the H_2O_2-treated cytochrome *c* oxidase. Schultz et al. (*26*) have shown that the narrow first-derivative spectrum from compound I of HRPC is the central portion of a much broader (1800 G) and weaker spectrum that can be detected using rapid passage conditions. The EPR spectrum of C*c*P, recorded at 77 K exhibits, a broad, isotropic line shape similar to that of the broad cytochrome *c* oxidase component but with a smaller line width, ΔHptp = 28 G. However at lower temperatures the EPR spectrum of C*c*P appears axial (*27*) with ΔHptp $\cong$ 60 G. These line shapes are determined by the exchange coupling between the oxyferryl heme and the tryptophan radical (*27*), and therefore, a difference in this coupling could lead to a broader yet more isotropic line shape as is observed for the C*c*O radical. Such behavior could be indicative of an increased radical to heme distance in C*c*O relative to C*c*P, although a change in the relative orientation of the radical and heme might also be affecting the strength of coupling. No other radical species giving rise to isotropic line shapes, line widths of this magnitude, and lacking partially resolved hyperfine structure as the radicals from C*c*O and C*c*P do has been reported.

Using temperature and microwave power variation it was possible to obtain separate ENDOR spectra from each of the two radical components of the H_2O_2-treated C*c*O EPR spectrum. Figure 2a shows the ENDOR spectrum of the narrow component obtained using high temperatures (100−120 K) and low microwave power (3.9 mW). This ENDOR spectrum was only obtainable within the field range covered by the narrow component of the EPR spectrum (i.e. could not be obtained at magnetic field positions where only the broad component was present). Figure 2b shows the spectrum of the broad component obtained at low temperature (12 K) and high microwave power (24 mW). This spectrum was obtainable over the field range covered by the EPR spectrum of the broad component (i.e. not just the region of the narrow component), although the ENDOR spectra shown were obtained at the center field of the EPR spectrum. This spectrum disappears above 20 K, and no microwave or rf

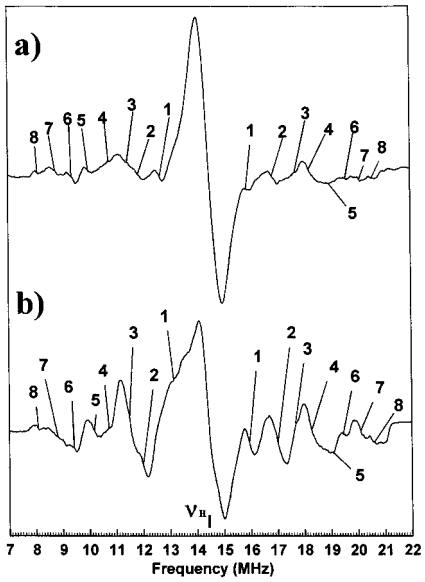

FIGURE 3: ENDOR spectra of H_2O_2-treated (a) cytochrome *c* oxidase (C*c*O) at pH 6.5 showing the spectrum arising from the narrow EPR signal and (b) horseradish peroxidase (HRPC). Numbers refer to features described in the text and Table 1. Conditions: microwave power 3.9 mW; rf power 100 W; rf modulation depth 177 kHz; average of 120 scans ((b) average of 80 scans); temperature 100 K.

powers which allowed its observation could be found above this temperature. Note that neither ENDOR spectrum could be detected outside the region of the broad and narrow radicals. This confirms what is clear from the spectra, that neither arises from the paramagnetic Cu_A(II) species. Several distinct features can be observed in each spectrum, but none is common to both confirming that the broad and narrow radicals arise from distinct chemical species. This is obviously supported by the temperature dependence of the ENDOR response and the different microwave power saturation behavior observed for the two radicals (*11, 19*). Note that the ENDOR spectrum of the narrow component was scanned over a smaller radio frequency range than that of the broad species. The ENDOR spectrum of the narrow component is necessarily weaker than that of the broad component (due to the higher temperatures and lower microwave powers required for optimum observation). To extend the scan range for the narrow component to that used for the ENDOR spectrum of the broad component while maintaining a sensible scan rate would have rendered the accumulation time for this spectrum unacceptably long.

Since H_2O_2 treatment of other heme proteins produces EPR spectra of free radicals similar to those observed in C*c*O (Figure 1), we can use ENDOR spectra of these radicals to aid assignment of the oxidase ENDOR spectra. Figure 3 shows a comparison of the ENDOR spectra derived from the narrow oxidase EPR signal and that of the porphyrin cation radical of HRPC. A majority of spectral features are common to both spectra and have identical or very similar hfcs. The hfcs measured here for the HRPC radical are in good agreement with those published previously (*28*). Any deviations presumably arise from the differences in the temperatures and methods of detection employed in this study and ref 28. Hfcs and tentative assignments for the C*c*O radical and the HRPC porphyrin cation radical are given in Table 1 together with the hfcs reported in ref 28. Since the

Table 1: Hyperfine Coupling Constants and Assignments for the Narrow Cytochrome *c* Oxidase (C*c*O) Derived Radical in Comparison with Those for Horse Radish Peroxidase (HRPC) Determined Here and by Roberts et al (*28*)

	hyperfine coupling (MHz)			
feature	C*c*O	HRPC	HRPC[a]	assgn
1	3.3	3.2	2.8	CH_2/vinyl
2	5.0	4.9	4.4	methyl
3	6.0	6.0	5.8	methyl
4	7.6	7.6		methyl
5	8.8	8.6	9.3	*meso* H
6	10.2	10.2		*meso* H
7	11.3	11.4	11.9	*meso* H
8	12.5	12.7		*meso* H

[a] Determined by Roberts et al. (*28*).

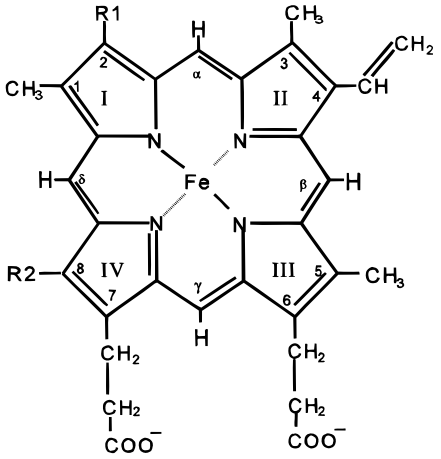

	R1	R2
Protoporphyrin IX	—CH=CH_2	—CH_3
Heme *a*	—CHOH($CH_2CH_2CHCCH_3$)$_3CH_3$	—CHO

FIGURE 4: Structure of heme *a* and protoporphyrin IX (heme *b*), with carbon atom-numbering scheme.

true width of the EPR spectrum of the HRPC radical (and therefore presumably the C*c*O radical) is approximately 1800 G (width at half-height) (*26*), these ENDOR spectra arise from only from the limited set of orientations of the radicals in the powder sample that contribute to the EPR spectrum at the observation field (orientation selection effect) (*29*). The most intense features in the ENDOR spectra of porphyrin radicals arise from hfcs to methyl groups β to the delocalized π system (*30*) (see Figure 4 for structures). Such methyl group hfcs have only small anisotropies (*30*) and so are minimally affected by the orientation selection effect. Furthermore, due to these small anisotropies, the measured hfcs approximate to the isotropic hfcs (A_{iso}) for the methyl groups. Extended Hückel calculations (*31*) and more recent density functional theory (DFT) calculations (*32*) suggest that the cation radical is created by the loss of an electron from the porphyrin a_{2u} orbital (although this may not be a pure state but admixed with an a_{1u} orbital contribution). As a consequence of this, the four methyl groups of the protoporphyrin IX cofactor of HRPC should give rise to resolved features in the ENDOR spectrum. These are visible as features 2−4 in Figure 3. One of the methyl group features is therefore not resolved, probably because it has the same hfc as another. This conclusion is supported by the Hückel

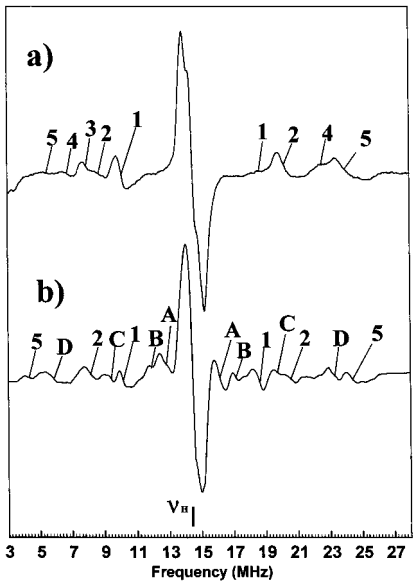

FIGURE 5: ENDOR spectra of H_2O_2-treated: (a) cytochrome *c* oxidase (C*c*O) at pH 6.5 showing the spectrum arising from the broad EPR signal and (b) cytochrome *c* peroxidase (C*c*P). Numbers and letters refer to features described in the text and in Table 2. Conditions: (a) microwave power 24 mW, rf power 100 W, rf modulation depth 140 kHz, average of 60 scans, temperature 12 K; (b) microwave power 15.9 mW, rf power 100 W, rf modulation depth 177 kHz, average of 80 scans, temperature 9 K.

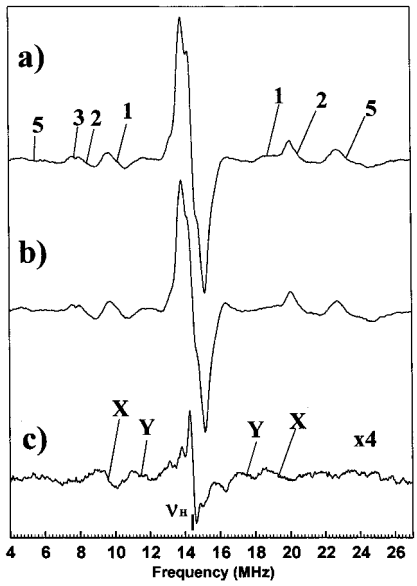

FIGURE 6: ENDOR spectra of H_2O_2-treated cytochrome *c* oxidase at pH 8.5 (0.1 M Tricine) showing the spectrum arising from the broad EPR signal: (a) incubated in H_2O buffer; (b) incubated in D_2O buffer; (c) the difference spectrum (a) minus (b). Letters refer to features described in the text and in Table 2. Conditions: microwave power 24 mW; rf power 100 W; rf modulation depth 140 kHz; average of 100 scans; temperature 12 K.

and DFT calculations (*31*, *32*), which suggest all four methyl groups should have similar hfcs. The heme A cofactor of C*c*O has only three methyl groups (Figure 4) and therefore can give rise to only three methyl group features in the ENDOR spectrum. The assumption of an a_{2u} state suggests, together with their lower intensities, that remaining features in the spectra of Figure 3 arise from the *meso* protons on the bridging carbon atoms (α, β, γ, δ, in Figure 4) (*28*, *31*, *32*). The hfcs to such protons have large anisotropies; therefore, the hfcs measured from the observed features are subject to the orientation selection effect and do not correspond to a defined component (A_x, A_y, or A_z) of the hfc. Note that there is no definitive assignment (based, for example, on specific deuteration) available for porphyrin cation radicals.

The line shape of the broad C*c*O radical EPR signal is similar to that exhibited by H_2O_2-treated C*c*P, Figure 1. The ENDOR spectra of the C*c*O and C*c*P radicals are shown in Figure 5. There are marked differences in intensity in the C*c*O spectrum between features above and below the proton Larmor frequency, ν_H. This occurs because the relaxation of those protons giving rise to features with intense low-frequency components is dominated by mechanisms different from those with intense high-frequency components. Differences in relaxation mechanisms suggest differences in the location of the protons relative to the delocalized π orbital containing the unpaired electron. Therefore this different behavior may indicate that the spectrum shows hfcs to both ring protons and β-CH_2 protons. Features 1, 2, and 5 are common to both spectra. Features 2 and 5 have been assigned to the β-CH_2 protons of a oxyferryl heme-coupled tryptophan (W191) cation radical in C*c*P (*33*) (see below for further discussion). As above, exchange coupling to the oxyferryl heme leads to orientation selection in the ENDOR spectrum, but since the β-CH_2 proton hfcs have small anisotropies, they are not particularly affected by orientation selection. However, the observed hfcs for the tryptophan radical ring protons depend on the orientation of the ring relative to the field direction. The field setting at the center of the EPR signal corresponds to a direction parallel to the Fe^{IV}=O bond of the oxyferryl heme (*33*). Since there are no tryptophan residues in the bovine heart C*c*O having orientations relative to heme *a* or a_3 (from the mechanism of action of the C*c*O a_3 is obviously preferred as a source of the oxyferryl species) similar to that of the radical-bearing W191 in C*c*P, there will be no correspondence between ring proton hfcs in the two radicals. Thus comparison of these spectra, while indicating that a tryptophan cation radical is formed in the two systems, is not conclusive evidence for the formation of a tryptophan cation radical in C*c*O.

Further evidence for the existence of a tryptophan cation radical can be obtained from H_2O/D_2O exchange experiments. Experimental and theoretical studies of such radicals show that they have large hfcs to the N(1) proton (*33*−*36*), which will exchange with a solvent deuteron. A difference spectrum constructed by subtracting a spectrum recorded in D_2O from one taken in H_2O is shown in Figure 6. These spectra were recorded on samples prepared at pH 8.5/pD 8.5 in order to maintain the oxidase in the "fast" form during the incubation of the enzyme in D_2O (see Materials and Methods). As a result they are not identical to the spectra of Figures 2 and 5. The main differences in the hfcs to the β-CH_2 protons (features 2 and 5) between the spectra shown in Figure 6 and Figures 2/5 are caused by the pH differences between the samples used and arise from a 1° change in the orientation of the tryptophan ring relative to the β-CH_2 protons (see below). Feature 4 seen in spectra at pH 6.5 is hidden under feature 5 at pH 8.5.

The difference spectrum shows two features X and Y. These are more obvious in the original H_2O spectrum (Figure

Table 2: Hyperfine Coupling Constants and Assignments for the Broad Cytochrome *c* Oxidase (C*c*O) Derived Radical in Comparison with Those for Cytochrome *c* Peroxidase (C*c*P) Determined Here and by Huyett et al. (*33*)[a]

	hyperfine coupling (MHz)				
feature	C*c*O	C*c*O(pH 8.5)	C*c*P	C*c*P[b]	assgn
A			3.3		?
B		4.2?	5.2	5.0	ring C(6)H orC(8)H
1	**8.6**	**8.6**	**8.4**		**ring C(5)H**
C			10.3		?
2	**11.4**	**12.0**	**12.4**	**13.0**	**β-CH_2 A_{iso}**
3	**13.0**	**12.2**			**ring C(7)H**
4	**15.2**	*c*		**15.0?**	**ring C(2)H**
D			17.6	16.0	ring N(1)H
5	**18.8**	**17.4**	**20.0**	**21.0**	**β-$CH_2$$A_{iso}$**
X		**9.8**			**ring N(1)H**
Y		**6.0**			**?**

[a] C*c*O assignments in bold type. [b] Huyett et al. (*33*). [c] Hidden under 5 at this pH.

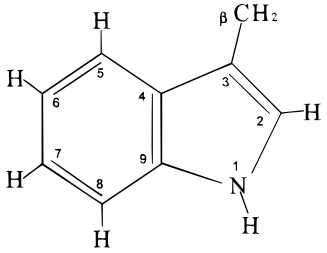

FIGURE 7: Structure and carbon/nitrogen atom-numbering scheme for tryptophan.

6a) on the right-hand side since X and Y are obscured by the greater prominence of Features 1 and 2 on the left-hand side. Feature, X, with an apparent hfc of 9.8 MHz, is consistent with the existence of an hfc to the exchangeable N(1)H of a tryptophan cation radical. The weaker feature Y, with an hfc of 6.0 MHz, arises from a protein or solvent proton within hydrogen-bonding distance of the radical, though not necessarily hydrogen bonded to it (see Discussion). The features in the difference spectrum that occur around the proton Larmor frequency, ν_H, arise from hfcs to exchangeable protons in the tryptophan radical environment but outside hydrogen-bonding distance.

The hfcs determined here for the C*c*O radical, the C*c*P tryptophan cation radical and the hfcs determined in (*33*) for the C*c*P radical are collected in Table 2, together with suggested assignments. The assignments are based on recent density functional calculations (*34*−*36*) on tryptophan cation radicals and similar model systems which have superseded the Hückel−McLachlan method (*33*). Differences between the hfcs measured in ref 33 and here for C*c*P probably arise from the use of Q-band (∼35 GHz microwave frequency) ENDOR in ref 33 which allows for the selection of a smaller subset of orientations and also from the differences in the experimental temperature (our spectrometer is incapable of the 2 K employed in ref 33). The structure and atom numbering scheme for tryptophan is shown in Figure 7.

DISCUSSION

Distinct ENDOR spectra have been obtained from the two components of the EPR spectrum of H_2O_2-treated C*c*O. ENDOR spectroscopy shows that the component giving rise to the narrow EPR signal arises from the A_{2u} state (or an A_{2u} dominated admixture of states) of a porphyrin cation radical spin coupled to an oxyferryl Fe^{IV}═O state. Therefore the obvious assignment is as an exchange coupled cation radical of the oxygen binding heme a_3. Similar EPR and ENDOR spectra have been shown to arise from an exchange coupled porphyrin (in this case protoporphyrin IX) cation radical in HRPC (Figures 1 and 3). The magnitude of the exchange coupling in such systems correlates with the nature of the proximal axial ligand to the heme iron and its effects on orbital symmetry (*14*). Since both heme a_3 and the heme cofactor of HRPC have proximal histidine residues coordinated to the iron, it is expected that they should have similar coupling and hence EPR and ENDOR properties (the effect on the ENDOR spectra of the different number of methyl groups in the two hemes has been discussed in the Results section above). The spin coupling in HRPC is very weak ($J \sim 0$) due to a fortuitous balance between ferromagnetic and antiferromagnetic coupling terms (*14*, *26*). This also seems to be the situation in cytochrome *c* oxidase given the formation of an A_{2u} state radical cation and the similarity to HRPC in the narrow EPR spectrum. Larger exchange coupling would lead to a more anisotropic line shape and displacement of the spectrum from the $g = 2.00$ region (*14*, *26*). It may be that the small exchange coupling has allowed us to detect ENDOR spectra of such coupled heme radical cations at higher temperatures than previously reported, though it is evident from Table 1 that our data do not differ much from those previously reported for HRPC at lower temperatures (*28*). The small differences between our data and those of Roberts et al. (*28*) for HRPC probably arise from differences in the temperatures at which the ENDOR spectra were acquired. The amount of porphyrin cation radical produced cannot be estimated from the EPR spectra, which are the result of two overlapping signals (*19*). However by analogy with HRPC the observation of any narrow radical at $g = 2.00$ (as part of a much broader spectrum) suggests the generation of a reasonable amount of porphyrin cation, and yet optical changes reported do not result in the loss in Soret intensity together with a broadening and blue-shift which might be expected if such a radical was formed. This inconsistency remains to be resolved, but it should be noted that there is not at the moment any clear correlation between optically detected intermediates and the amount of these EPR radicals (*19*).

Comparison with the EPR and ENDOR spectra previously obtained for H_2O_2-treated C*c*P (Figures 1 and 5) (*16*, *27*, *33*) suggests that the broad component of the C*c*O EPR spectrum arises from a tryptophan cation radical. Both the C*c*P and C*c*O radicals have similar hfcs to β protons, and both have large hfcs to an exchangeable proton (see Table 2 and ref 33). However, the assignment of the radical formed in C*c*P has itself been questioned by Krauss and Garmer (*37*), who favor a tautomeric form of the neutral tryptophan radical on the basis of optical studies.

The assignment of the radical formed in C*c*O as a tryptophan cation radical is supported by several properties of the ENDOR spectrum. The Heller and McConnell equation for an aromatic radical is (*38*):

$$A_{iso}(H_\beta) \cong \rho_c^{\pi} [B' + B \cos^2 \theta]$$

where $A_{iso}(H_\beta)$ is the isotropic hfc to a proton of the β-CH_2

group, ρ_c^{π} is the π spin density at the ring carbon of the radical to which the β-CH_2 group is attached, B' and B are numerical constants, B' being negligible and B being equal to 162 MHz, and θ is the angle between the normal to the aromatic ring plane and the C(β) to H(β) bond. Using this equation and the data of Table 2 for the oxidase radical gives $\rho_c^{\pi} = 0.37$ and $\theta = 55.9°$ for feature 5 and $\theta = 64.1°$ for feature 2. Likewise for the tryptophan cation radical (W191) of C*c*P $\rho_c^{\pi} = 0.39$ and $\theta = 56.1°$ for feature 5 and $\theta = 63.9°$ for feature 2. This agrees well with previously reported data for this radical (*33*), $\theta = 56°$ (and 64°) and an average $\rho_c^{\pi} = 0.39$ (theoretical calculations give similar values between 0.3 and 0.4, e.g. refs 35 and 37). Unfortunately, this value of ρ_c^{π} is not diagnostic of a tryptophan cation radical. Tryptophan neutral radicals (having no proton at N(1), such as those observed in the *E. coli* ribonucleotide reductase R2 Y122F mutant (*39*)) and tyrosine neutral radicals (which have been studied in vitro, e.g. ref 40, and in biochemical systems such as photosystem 2 (*41*) and ribonucleotide reductase (*42*)) both have similar values of ρ_c^{π}. However, this value does exclude the less well studied tyrosine cation (*43*) and histidine (*44*) radicals, which have higher ρ_c^{π} than determined here, although the existing experimental data on these radicals are far from complete.

Second there is the 9.8 MHz hfc to the exchangeable proton, labeled X in Table 2. Such an hfc is observed in C*c*P (labeled Feature D in Table 2) (*33*) (although the apparent magnitude of the hfc is different because of the orientation selection effect, as described in Results) and is predicted by theoretical calculations (*34*−*36*) for tryptophan cation radicals. No such large hfcs to exchangeable protons have been observed in studies of tryptophan neutral radicals (*39*) or tyrosine neutral radicals (*41, 42*) in biological systems, nor are they predicted by theoretical studies of such radicals (*35, 36, 45*). Smaller hfcs to exchangeable protons have been reported for the tryptophan neutral radical $W_a^{\bullet}$ (W111) in the R2 Y122F mutant of *E. coli* ribonucleotide reductase (largest component, A_{11}, of a rhombic hfc = 5.4 MHz) (*39*) and the neutral tyrosine radical $Y_D^{\bullet}$ of photosystem 2 ($A_{||} \cong 6.2$ MHz) (*46*). These hfcs have been assigned to protons hydrogen bonded to N(1) of the tryptophan radical (*39*) and the oxygen atom of the tyrosine radical (*46*), although such studies only determine distances and do not prove the existence of hydrogen bonds. Feature Y of Figure 6c may arise from such an exchangeable proton within hydrogen-bonding distance of the tryptophan radical in C*c*O. Note that the lack of a large hfc to an exchangeable proton was taken as evidence for the formation of a neutral radical, rather than a cation radical, in ref 39. Therefore, considered together with the calculation of ρ_c^{π}, the large hfc to an exchangeable proton demonstrates that the broad component of the EPR spectrum of H_2O_2-treated C*c*O arises from a tryptophan cation radical exchange coupled to the oxyferryl Fe^{IV}=O state of heme a_3. The formation of a tryptophan radical on treatment of C*c*O with H_2O_2 (at pH 8.8−9.0) has also been suggested by optical measurements (*7*). A recent EPR spin-trapping study (*47*) shows the formation of a cysteine-based thiyl radical with excess H_2O_2 at pH 7.4. This is clearly inconsistent with the data presented here but probably indicates that a cysteine thiyl radical is the first or most stable radical formed under these conditions that is accessible to the 5,5-dimethyl-1-pyrroline *N*-oxide (DMPO) trapping molecule. A tyrosine radical was also trapped in the recent spin-trapping work (*47*) but only after extensive modification of the protein with the cysteine blocking reagent *N*-ethylmaleimide. A tyrosine radical has been identified in the H_2O_2-treated cytochrome *c* oxidase from the bacterium *Paracoccus denitrificans* (*21*) using specific deuteration and EPR spectroscopy. The EPR line shape and limited number of hfcs reported in that study show clearly that this tyrosine radical is not related to the radicals observed by us here (see also ref 19) or by Fabian and Palmer (*11*) in beef heart cytochrome *c* oxidase. The different radicals observed in the two different oxidases when treated with H_2O_2 may result from interspecific differences, although in the absence of data characterizing the chemical species formed by treatment of *P. denitrificans* oxidase with H_2O_2 definitive comparison of the two systems is not possible. We have prepared samples of bovine cytochrome *c* oxidase under conditions identical to those used to produce the tyrosine radical in ref 21, using a concentration of H_2O_2 equimolar with C*c*O at a pH of 6.0 and freezing the sample immediately. These samples contained the narrow and broad EPR signals observed after treatment with 1 mM H_2O_2 (Figure 1) but at much lower concentrations. We do not therefore attribute the differences between our results and those reported in ref 21 to differences in sample preparation.

The information derived from the ENDOR spectrum can be used to suggest which tryptophan residue around the binuclear center of bovine C*c*O gives rise to the radical. There are two conserved tryptophan residues where the radical bearing rings are within 10 Å of the iron atom of heme a_3, W126 and W236 (*17, 48*) (see Brookhaven Protein Database entry 2OCC.PDB). The X-ray crystal structure provides approximate values of $\theta = 52°$ for W126 and $\theta = 44°$ for W236. Furthermore there is no obvious countercharge for the tryptophan cation in the vicinity of W236, while W126 is within ∼3.5 Å of a negatively charged heme a_3 propionate group. Thus the assignment of the location of the tryptophan cation radical to W126 is more consistent with both the crystallographic and ENDOR data than an assignment of the cation to W236. Note that both W126 and W236 are ∼9 Å from the heme a_3 iron, whereas W191 in C*c*P is only ∼5 Å (at closest approach of the ring) from the iron. This may explain the apparent differences in the exchange coupling and the shape of the EPR spectra of the oxidase and C*c*P radicals.

Ascorbate peroxidase is a heme-containing enzyme which shares 33% global sequence identity and a very similar active site structure with C*c*P (*49*). Although C*c*P W191 is conserved in ascorbate peroxidase (as W179), it does not form a cation radical in the latter enzyme; instead a porphyrin cation radical is formed at the heme. A recent theoretical study (*50*) has suggested that differences in electrostatic interactions between the proximal histidine ligand to the heme iron, the radical-forming (in C*c*P) tryptophan, and a nearby aspartic acid residue may control the location of the radical state. However, the structure around the heme a_3 binding site of C*c*O is very different to that of C*c*P or ascorbate peroxidase (e.g. the conserved tryptophan residues in the oxidase are on the distal side of the heme and not the proximal side as are W191 in C*c*P and W179 in ascorbate peroxidase), and therefore, such a mechanism is unlikely to be controlling radical location in cytochrome *c* oxidase.

Definition of the number and identity of radical species associated with oxidase intermediates is an important step in understanding its mechanism, particularly as such radicals could be linked to protonation changes that are integral to the mechanism by which electron transfer is coupled to proton translocation. Indeed, models have been elaborated recently (*9*, *18*, *19*−*21*) in which a tyrosine radical species plays a key role in coupled protonation events, and MacMillan et al. (*21*) report the presence of a tyrosine radical in the **F**• intermediate of the homologous cytochrome oxidase of *Paracoccus denitrificans*. However, if its role is critical, then this same radical might be expected to be detected in all members of the oxidase superfamily. The data presented here and in previous publications (*11*, *19*) indicate that this is not the case. Hence, the alternative possibility must be considered that, although radical species can be associated with some oxygen intermediates, the pattern is not always the same. In this case, the role of such radicals may not be central to protonmotive mechanism but rather to act as one contributing factor to the general stability of the transient catalytic intermediates.

ACKNOWLEDGMENT

We gratefully acknowledge Jonathan Ramsey for technical assistance and Fraser MacMillan for sending us a copy of his manuscript prior to publication.

REFERENCES

1. Wikström, M. (1981) *Proc. Natl. Acad. Sci. U.S.A. 78*, 4051−4054.
2. Wikström, M. (1988) *Chem. Scr. 28A*, 71−74.
3. Wikström, M., and Morgan, J. (1992) *J. Biol. Chem. 267*, 10266−10273.
4. Wrigglesworth, J. M. (1984) *Biochem. J. 217*, 715−719.
5. Kumar, Ch., Naqui, A., and Chance, B. (1984) *J. Biol. Chem. 259*, 11668−11671.
6. Vygodina, T., and Konstantinov, A. (1989) *Biochim. Biophys. Acta 973*, 390−398.
7. Weng, L., and Baker, G. M. (1991) *Biochemistry 30*, 5727−5733.
8. Proshlyakov, D. A., Ogura, T., Shinzawa-Itoh, K., Yoshikawa, S., and Kitagawa, T. (1996) *Biochemistry 35*, 8580−8586.
9. Proshlyakov, D. A., Pressler, M. A., and Babcock, G. T. (1998) *Proc. Natl. Acad. Sci. U.S.A. 95*, 8020−8025.
10. Ogura, T., Hirota, S., Proshlyakov, D. A., Shinzawa-Itoh, K., Yoshikawa, S., and Kitagawa, T. (1996) *J. Am. Chem. Soc. 118*, 5443−5449.
11. Fabian, M., and Palmer, G. (1995) *Biochemistry 34*, 13802−13810.
12. Patterson, W. R., Poulos, T. L., and Goodin, D. B. (1995) *Biochemistry 34*, 4342−4345.
13. Chuang, W.-J., and van Wart, H. E. (1992) *J. Biol. Chem. 267*, 13293−13301.
14. Benecky, M. J., Frew, J. E., Scowen, N., Jones, P., and Hoffman, B. M. (1993) *Biochemistry 32*, 11929−11933.
15. Karthein, R., Dietz, R., Nastainczyk, W., and Ruf, H. H. (1988) *Eur. J Biochem 171*, 321−328.
16. Sivaraja, M., Goodin, D. B., Smith, M., and Hoffman, B. M. (1989) *Science 245*, 738−740.
17. Yoshikawa, S., Shinzawa-Itoh, K., Nakashima, R., Yaono, R., Yamashita, E., Inoue, N., Yao, M., Fei, M. J., Libeu, C. P., Mizushima, T., Yamaguchi, H., Tomizaki, T., and Tsukihara, T. (1998) *Science 280*, 1723−1729.
18. Ostermeier, C., Harrenga, A., Ermler, U., and Michel, H. (1997) *Proc. Natl. Acad. Sci. U.S.A. 94*, 10547−10553.
19. Jünemann, S., Heathcote, P., and Rich, P. R. (2000) *Biochim. Biophys. Acta 1456*, 56−66.
20. Brittain, T., Little, R. H., Greenwood, C., and Watmough, N. J. (1996) *FEBS Lett. 399*, 21−25.
21. MacMillan, F., Kannt, A., Behr, J., Prisner, T., and Michel, H. (1999) *Biochemistry 38*, 9179−9184.
22. Moody, A. J., Cooper, C. E., and Rich, P. R. (1991) *Biochim. Biophys. Acta 1059*, 189−207.
23. Rich, P. R., and Moody, A. J. (1997) Cytochrome *c* oxidase. In *Bioelectrochemistry: principles and practice* (Gräber, P., and Milazzo, G., Eds.) pp 419−456, Birkhäuser Verlag AG, Basel.
24. Bergmeyer, H. U., Gawehn, K., and Grassl, M. (1970) in *Methoden der Enzymatischen Analyse* (Bergmeyer, H. U., Ed.) p 40, Verlag Chemie, Weinheim, Germany.
25. Yonetani and Ray (1965) *J. Biol. Chem. 240*, 4503−4514.
26. Schulz, C. E., Devaney, P. W., Winkler, H., Debrunner, P. G., Doan, N., Chiang, R., Rutter, R., and Hager, L. P. (1979) *FEBS Lett. 103*, 102−105.
27. Hoffman, B. M., Roberts, J. E., Kang, C. H., and Margoliash, E. (1981) *J. Biol. Chem. 256*, 6556−6564.
28. Roberts, J. E., Hoffman, B. M., R., Rutter, R., and Hager, L. P. (1981) *J. Biol. Chem. 256*, 2118−2121.
29. Rist, G. H., and Hyde, J. S. (1970) *J. Chem. Phys. 52*, 4633−4643.
30. Norris, J. R., Scheer, H., and Katz, J. J. (1979) in *The Porphyrins* (Dolphin, D., Ed.) Vol. 4, pp 159−195, Academic Press, New York.
31. Hanson, L. K., Chang, C. K., Davis, M. S., and Fajer, J. (1981) *J. Am. Chem. Soc 103*, 663−670.
32. Kuramochi, H., Noodleman, L., and Case, D. A. (1997) *J. Am. Chem. Soc 119*, 11442−11451.
33. Huyett, J. E., Doan, P. E., Gurbiel, R., Houseman, A. P., Sivaraja, M., Goodin, D. B., Smith, M., and Hoffman, B. M. (1995) *J. Am. Chem. Soc. 117*, 9033−9041.
34. O'Malley, P. J., and Ellson, D. A. (1996) *Chem. Phys. Lett. 260*, 492−498.
35. Walden, S. E., and Wheeler, R. A. (1996) *J. Phys. Chem. 100*, 1530−1535.
36. Himo, F., and Eriksson, L. A. (1997) *J. Phys. Chem. B 101*, 9811−9818.
37. Krauss, M., and Garmer, D. R. (1993) *J. Phys. Chem. 97*, 831−836.
38. Heller, H. C., and McConnell, H. M. (1960) *J. Chem. Phys. 32*, 1535.
39. Lendzian, F., Sahlin, M., MacMillan, F., Bittl, R., Fiege, R., Pöysch, S., Sjöberg, B.-M., Gräslund, A., Lubitz, W., and Lassmann, G. (1996) *J. Am. Chem. Soc. 118*, 8111−8120.
40. Hulsebosch, R. J., van den Brink, J. S., Nieuwenhuis, S. A. M., Gast, P., Raap, J., Lugtenburg, J., and Hoff, A. J. (1997) *J. Am. Chem. Soc. 119*, 8685−8694.
41. Rigby, S. E. J., Nugent, J. H. A., and O'Malley, P. J. (1994) *Biochemistry 33*, 1734−1742.
42. Bender, C. J., Sahlin, M., Babcock, G. T., Barry, B. A., Chandrashekar, T. K., Salowe, S. P., Stubbe, J., Lindström, B., Petersson, L., Ehrenberg, A., and Sjöberg, B.-M. (1989) *J. Am. Chem. Soc. 111*, 8076−8083.
43. Box, H. C., Budzinski, E. E., and Freund, H. G. (1974) *J. Phys. Chem. 61*, 2222−2226.
44. Lassmann, G., Eriksson, L. A., Himo, F., Lendzian, F., and Lubitz, W. (1997) *J. Phys. Chem. A 103*, 1283−1290.
45. O'Malley, P. J., and Ellson, D. (1997) *Biochim. Biophys. Acta 1320*, 65−72.
46. Tang, X.-S., Zheng, M., Chisholm, D. A., Dismukes, G. C., and Diner, B. A. (1996) *Biochemistry 35*, 1475−1484.
47. Chen, Y.-R., Gunther, M. R., and Mason, R. P. (1999) *J. Biol. Chem. 274*, 3308−3314.
48. Tsukihara, T., Aoyama, H., Yamashita, E., Tomizaki, T., Yamaguchi, H., Shinzawa-Itoh, K., Nakashima, R., Yaono, R., and Yoshikawa, S. (1996) *Science 272*, 1136−1144.
49. Patterson, W. R., and Poulos, T. L. (1995) *Biochemistry 34*, 4331−4341.
50. Menyhárd, D. K., and Náray-Szarbó, G. (1999) *J. Phys. Chem. B 103*, 227−233.

BI992614Q